journal

J. Am. Ceram. Soc., **85** [4] 833–38 (2002)

B-Site Order–Disorder Transition in $Pb(Mg_{1/3}Nb_{2/3})O_3$–$Pb(Mg_{1/2}W_{1/2})O_3$ Triggered by Mechanical Activation

Xingsen Gao,[†] Junmin Xue,[†] Ting Yu,[‡] Zexiang Shen,[‡] and John Wang[*,†]

Department of Materials Science and Department of Physics, National University of Singapore, Singapore 119260

B-site cation order–disorder transition induced by mechanical activation was observed in $Pb(Mg_{1/3}Nb_{2/3})O_3$–$Pb(Mg_{1/2}W_{1/2})O_3$ (PMN–PMW) solid solution, which was examined using both XRD diffraction and Raman spectroscopic study. The order–disorder transition is composition dependent. Mechanical activation triggers the B-site disordering, which can be steadily recovered by thermal annealing at elevated temperature, i.e., at temperatures around 600°C. Raman spectroscopy demonstrated that there existed tiny ordered microdomains in 0.4PMN·0.6PMW subjected to up to 20 h of mechanical activation, although they cannot be shown by X-ray diffraction. This is a result of the equilibrium between the mechanical destruction and temperature-facilitated recovering at the collision points during mechanical activation. It is therefore unlikely that a complete disordering can be realized in PMN–PMW by mechanical activation. The disordering in PMN–PMW triggered by mechanical activation occurs simultaneously with the refinement in crystallite size at the initial stage of mechanical activation, suggesting that the fragmentation of crystallites is responsible for the order–disorder transition at least during the initial stage of mechanical activation.

I. Introduction

B-site ordering in ferroelectric $Pb(B'B'')O_3$ of complex perovskite structure exhibits a strong effect on the dielectric, and ferroelectric, diffusive phase transitions.[1,2] Since the discovery of B-site ordering in $Pb(Sc_{1/2}Ta_{1/2})O_3$ (PST) in 1980,[1] extensive investigation has been made into the order–disorder transitions of various perovskite structures.[3–6] Recent studies using synchrotron radiation XRD,[7] NMR,[8] EPR,[9] Raman spectroscopy,[10] as well as modeling and simulation[11,12] have led to considerable understanding of the B-site ordering and its effects on the relaxor ferroelectric behavior. The order–disorder transition has been observed to be affected by B-site composition,[4–6] A-site vacancies,[13] and long-time annealing.[1,2,14] For example, disordered PST can be obtained by high-temperature quenching, and the ordering can be realized by a long-time annealing. In this paper, we report the order–disorder transition in $(1-x)$PMN·xPMW induced by mechanical activation, as studied using both XRD and Raman spectrometry.

Mechanical alloying, which was initially devised for the synthesis of alloys and metal compounds, has recently been extended to many other types of oxides, magnetic materials, and electronic materials.[15,16] Several mechanochemical reactions can be triggered, which may or may not be realized by conventional thermal activation.[17] Mechanical activation, which has been used to synthesize a number of novel materials having metastable and amorphous structures,[18,19] can trigger the order–disorder transition in Fe–Al alloys.[20,21] Several unique phenomena have been observed in association with the mechanical activation of complex perovskite structures. However, the order–disorder transition triggered by mechanical activation in relaxor ferroelectrics has not been studied in detail. In this work, we choose $Pb(Mg_{1/3}Nb_{2/3})O_3$–$Pb(Mg_{1/2}W_{1/2})O_3$ (PMN–PMW), which shows a long-range B-site ordering and is composition dependent,[22] to study the order–disorder transition triggered by mechanical activation.

II. Experiments

The starting materials used in this work were commercially available PbO (99% in purity, J. T. Baker, Inc.), MgO (99.6% in purity, J. T. Baker, Inc.), Nb_2O_5 (99% in purity, Aldrich, USA), and WO_3 (99.9% in purity, Aldrich, USA). Mechanical activation of columbite precursor was used to prepare pyrochlore-free relaxor ferroelectrics, as described in previous studies.[17] For this, $MgWO_4$ and $MgNb_2O_4$ were synthesized by calcination of mixed oxides of MgO and WO_3 or MgO and Nb_2O_5 at 1000°C for 6 h. The resulting powders were mixed with PbO together in the ratios as required by the stoichiometric composition of $(1-x)$PMN·xPMW. The powder mixtures were each subjected to mechanical activation for 10 h and then calcined at 900°C for 2 h, resulting in formation of $(1-x)$PMN·xPMW of perovskite structure, as shown in Fig. 1. They were mechanically activated for various time periods ranging from 0 to 20 h, to investigate the order–disorder phase transition triggered by mechanical activation. The activated samples were then subjected to thermal annealing at various temperatures, followed by studies using XRD and Raman spectroscopy.

For mechanical activation, each powder sample was loaded in a stainless vial 40 mm in diameter and 40 mm in length with one stainless steel ball 12.7 mm in diameter inside. On completion of mechanical activation, they were examined using an X-ray diffractometer for phase identification (Cu$K\alpha$, X′ per diffractometer, Phillips). The degree of long-range ordering was measured by comparing the intensity of the principal perovskite (200) peak with that of the supperlattice (111) peak. Crystallite size was determined using the Scherrer equation based on broadening of the (220) peak at a 2θ of 31.7°,[23] while the ordered domain size was calculated based on (111) superlattice peaks at about 19.4°. Micro-Raman spectra were acquired at room temperature in the backscattering geometry using a Spex T6400 single-grating Raman spectrometer with an Olympus microscope attachment and equipped with a liquid-nitrogen-cooled CCD detector. The relative degree of long-range ordering was calculated based on the intensity ratio of the band at around 384 cm^{-1} to that at 278 cm^{-1}, and the intensity ratio of band 841 cm^{-1} to 786 cm^{-1}. High-resolution electron microscopy (HRTEM, Philips CM 300 FEG) was used to study the crystallite structure of mechanically activated PMN–PMW compositions.

III. Results and Discussion

Figure 1 shows the XRD diffraction patterns of $(1-x)$PMN·xPMW calcined at 900°C for 2 h, each exhibiting a

S. E. Trolier-McKinstry—contributing editor

Manuscript No. 187591. Received July 12, 2001; approved December 13, 2001.
This work was supported by the National University of Singapore and the Institute of Materials Research and Engineering (IMRE).
*Member, American Ceramic Society.
[†]Department of Materials Science.
[‡]Department of Physics.

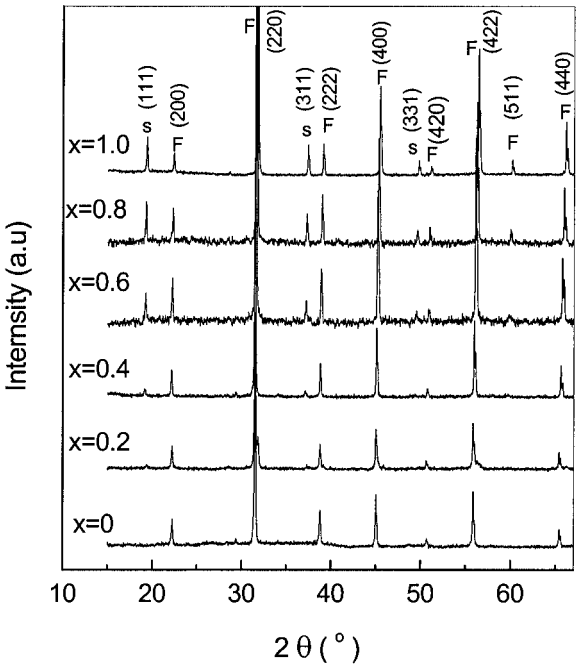

Fig. 1. XRD patterns of $(1-x)$PMN·xPMW solid solutions synthesized by mechanical activation for 20 h and consequently calcined at 900°C for 2 h, showing that they are single perovskite phases. "s" represents the supperlattice diffraction peaks, and "F" the principle diffraction peaks of perovskite.

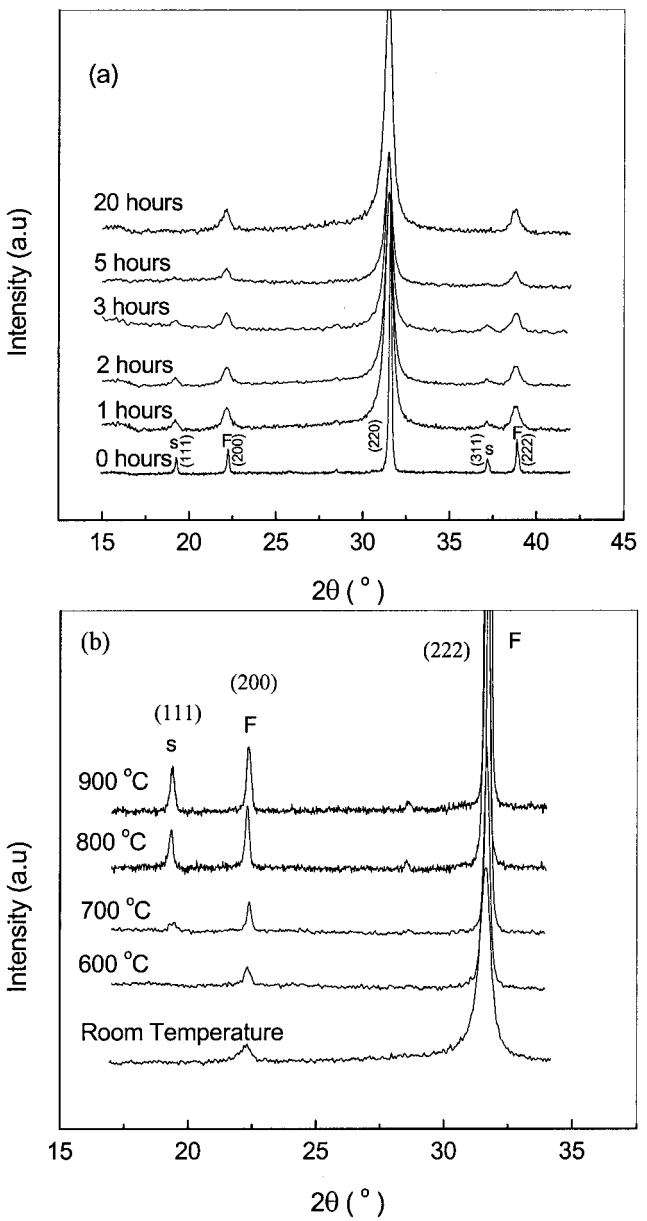

Fig. 2. XRD traces of 0.4PMN·0.6PMW solid solution (a) subjected to various periods of mechanical activation demonstrating the disappearance of the (111) superlattice diffraction pattern, and (b) consequently calcined at various temperatures exhibiting the recovering of the (111) superlattice diffraction peak.

well-established perovskite structure. In addition to the principal peaks of perovskite structure, the occurrence of B-site ordering, as indicated by the superlattice (111), (311), (331) peaks marked by "s", appears to be composition dependent. The superlattice structure occurs in the compositions of >0.2 PMW. Its relative intensity increases with increasing PMW content in PMN, which is in agreement with what was reported in a previous study.[22]

As shown in Fig. 1, 0.4PMN·0.6PMW is a typical composition exhibiting B-site ordering, which was chosen to study the order–disorder transition triggered by mechanical activation. The phase evolution of 0.4.PMN·0.6.PMW as a function of mechanical activation time is shown in Fig. 2(a). It exhibits a strong B-site ordering in the initial unactivated state, as shown by the (111) and (311) superlattice diffractions at around 2θ of 19.4° and 37.6°, respectively. The superlattice diffraction peaks decrease in intensity with increasing mechanical activation time. They undergo a significant peak broadening at the initial hour of mechanical activation and then fall fast in peak intensity with a further increase in mechanical activation time. This implies that the disordering is associated with the refinement in crystallite and ordered domain sizes. The superlattice diffraction peaks of (111) and (311) at 2θ of 19.4° and 37.6° had completely disappeared from the XRD trace after 5 h of mechanical activation. As expected, a steady recovery of ordering in 0.4PMN·0.6PMW is observed when the mechanically activated compositions are thermally annealed at an increased temperature as shown in Fig. 2(b). The apparent ordering starts to appear at around 700°C and the recovery is largely completed at 900°C.

Crystallite size and ordered domain size for the above 0.4PMN·0.6PMW composition, as a function of mechanical activation and thermal annealing, were calculated using the Scherrer equation as shown in Figs. 3(a,b). In Fig. 3(a), both the domain size and the crystallite size decrease dramatically at the initial hour of mechanical activation, followed by a fall in the decrease rate when mechanical activation is extended to more than 2.0 h. In fact, the calculated crystallite size and ordered domain size demonstrate a similar rate in size refinement at both the initial and late stages of mechanical activation. This shows that the refinement in crystallite and ordered domain sizes took place simultaneously at the initial stage of mechanical activation, and the order–disorder transition occurred when the crystalline size was refined enough. Figure 3(b) illustrates the crystallite and ordered domain sizes as a function of annealing temperature for the composition subjected to 20 h of mechanical activation. Both the crystallite and domain sizes increase sharply over the temperature range of 600° to 800°C. Little further change was observed above 800°C, where both the crystallite and ordered domain sizes have more or less recovered to those in the unactivated state. As discussed below based on the Raman spectroscopy, there existed tiny ordered microdomains in the mechanically activated PMN–PMW, although they could not be effectively detected by X-ray diffraction. This was supported by the study using high-resolution transmission electron microscopy. Figure 4 is a bright-field HRTEM micrograph for 0.4PMN·0.6PMW that was subjected to mechanical activation for 20 h. Nanocrystalline domains of perovskite structure and 7 to 12 nm in size were observed to occur in an amorphous matrix, which were highly defective.

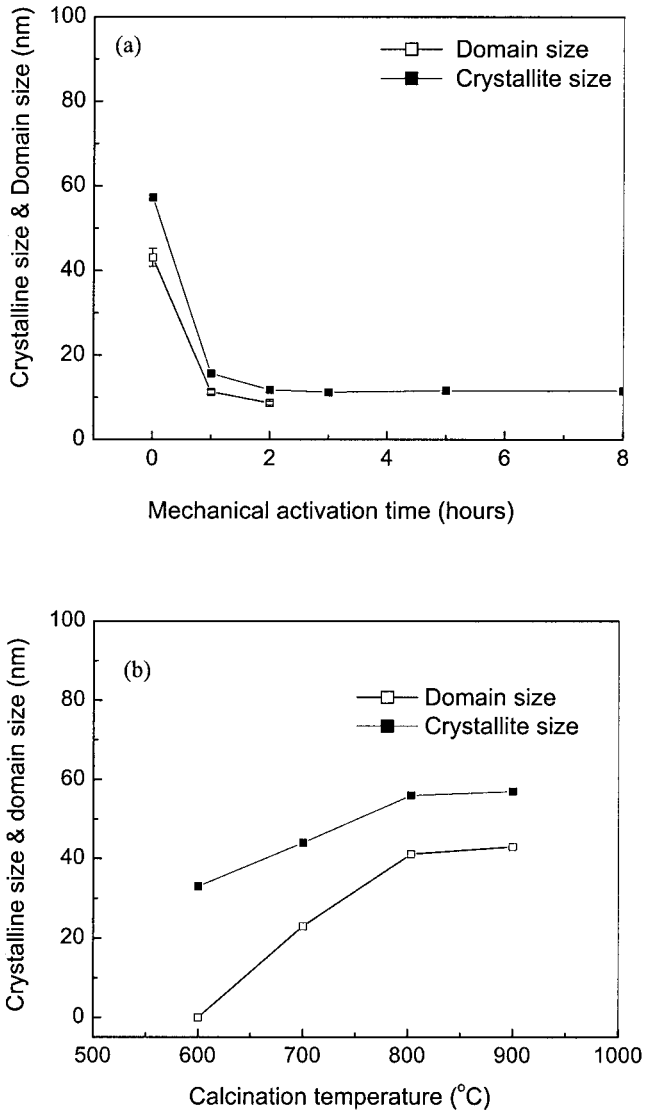

Fig. 3. Crystallite size and B-site ordering domain size for 0.4PMN·0.6PMW: (a) as a function of mechanical activation hours, and (b) as a function of calcination temperature.

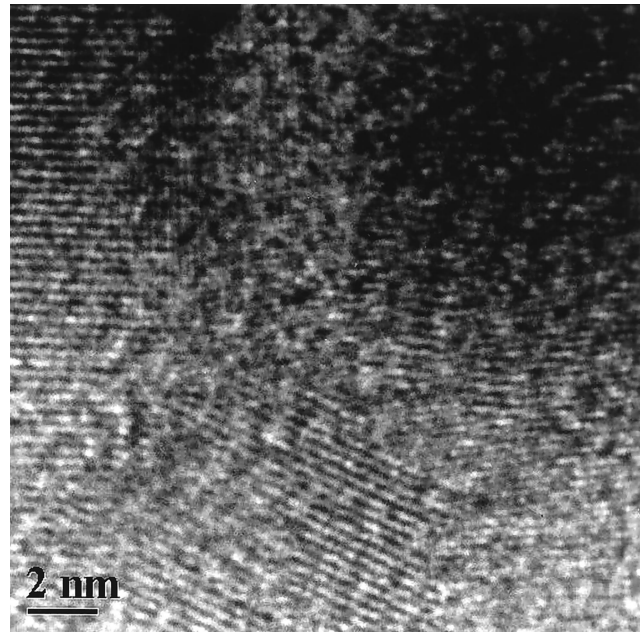

Fig. 4. HRTEM image of 0.4PMN·0.6PMW subjected to mechanical activation for 20 h.

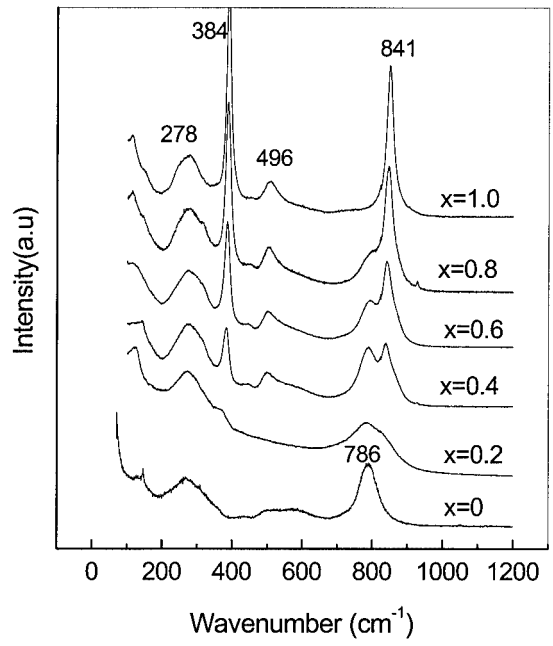

Fig. 5. Raman spectra of $(1-x)$PMN·xPMW solid solution of different compositions showing the intensity dependence of bands centered at 384 and 841 cm^{-1} on the content of PMW.

The Raman spectra of PMN–PMW, as a function of composition, are shown in Fig. 5. PMW exhibits the *Fm*3*m* group modes, which are similar to those of PST,[24,25] The bands at around 278 and 496 cm^{-1} can be attributed to the E mode or second-order modes. The Raman band at around 384 cm^{-1} can be ascribed to F_{2u}, which is caused by the B-site ordering, and therefore it can be used as an indication of the degree of B-site ordering.[24,25] Although the origin of PMN Raman spectra is still the subject of debate and discussion, it is commonly accepted that PMN belongs to the *Fm*3*m* group. Its high-frequency band at around 786 cm^{-1} is attributed to the A_{1g} mode, and the other bands are related to $E_g + T_{1u} + T_{2u}$ modes.[26,27] The band at around 384 cm^{-1} indicating the B-site ordering begins to appear in the compositions containing >0.2 PMW, and its intensity increases with increasing PMW content. With increasing PMW content in PMN, the band at around 786 cm^{-1} disappears gradually, and at the same time, the band centered at 841 cm^{-1} arises and increases in intensity due to the B-site ordering.

The Raman spectra of 0.4PMN·0.6PMW subjected to various mechanical activation durations are illustrated in Fig. 6(a), where the change in band intensity centered at 384 cm^{-1} clearly demonstrates that the degree of ordering decreases with increasing mechanical activation time. There is also an apparent shift of band at 786 cm^{-1} toward the one at 841 cm^{-1}, which undergoes a substantial degree of band broadening, with increasing mechanical activation time. This is in agreement with what has been indicated by the XRD. However, the Raman band at 384 cm^{-1} cannot be eliminated by extension of mechanical activation. Instead, its intensity decreases dramatically at the initial hour of mechanical activation and further extension in mechanical activation led to little change in the bandwidth and intensity. A similarly weak Raman band at around 384 cm^{-1} was reported by Reaney *et al.*[28] and Randall *et al.*,[29] in disordered PST quenched from an elevated temperature, where the B-site ordering domains below 3 nm were observed in TEM dark-field image; however, they were too small to be detected by XRD diffraction because of the broadening of the superlattice peaks. The broadened Raman peak at around 384

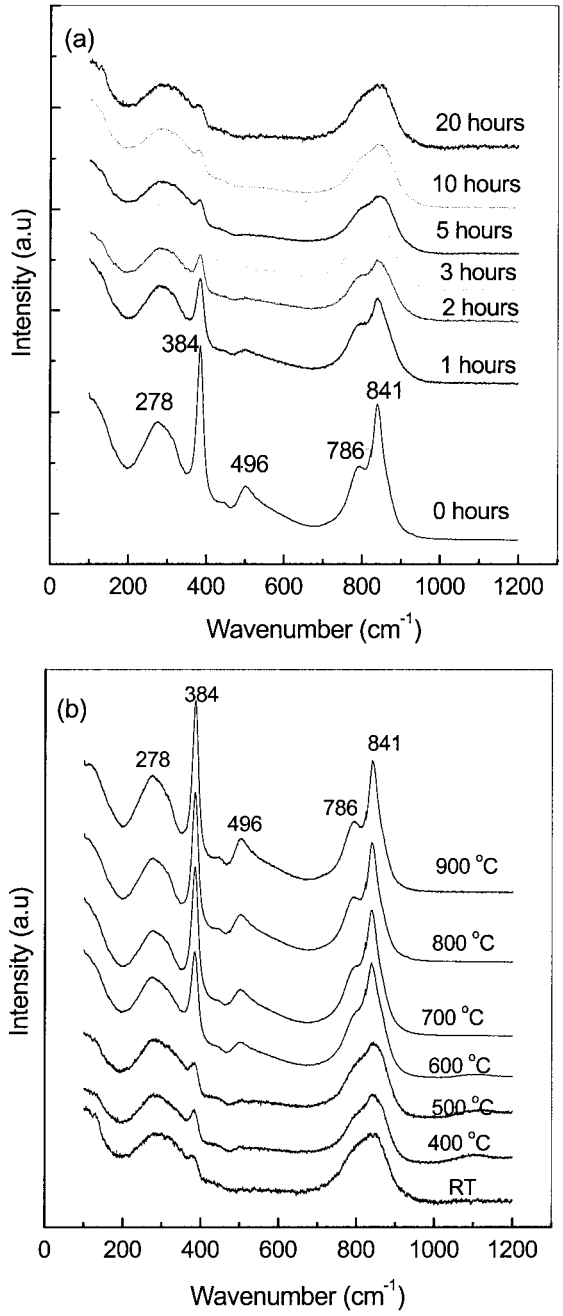

Fig. 6. Raman spectra of 0.4PMN·0.6PMW: (a) subjected to various periods of mechanical activation, and (b) calcined at different temperatures.

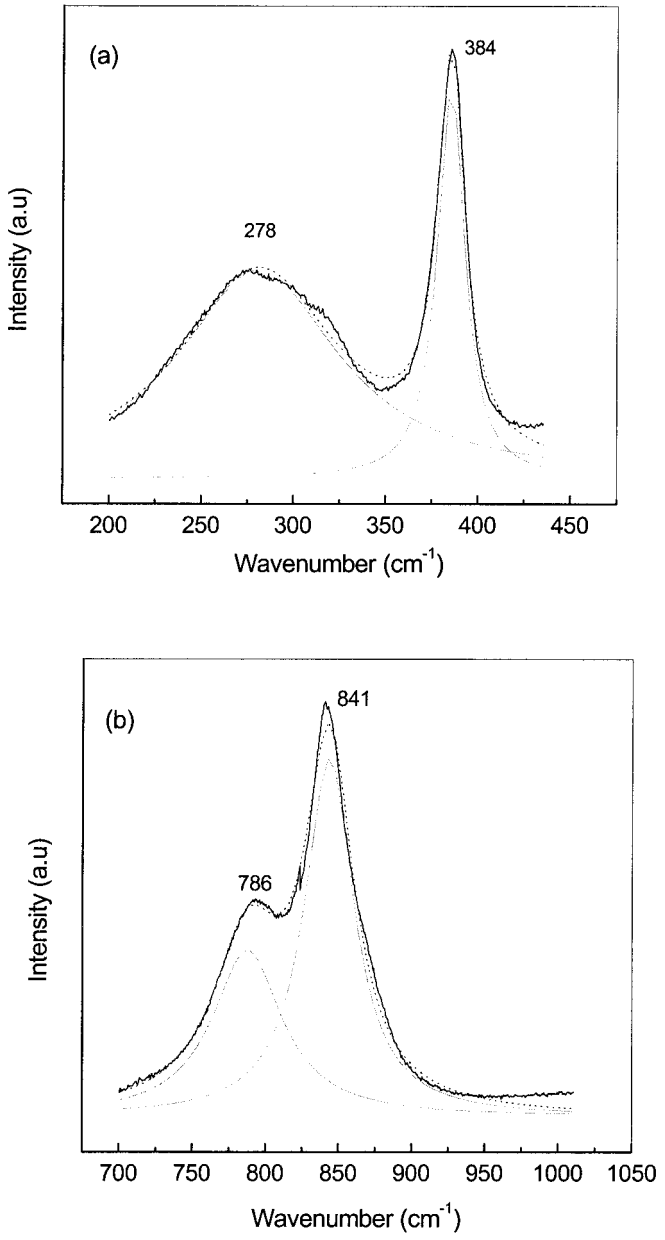

Fig. 7. Raman spectrum of 0.4PMN·0.6PMW showing deconvolution with superimposed Gaussian functions: (a) 200–450 cm^{-1} group of bands, (b) the 700–950 cm^{-1} group of bands.

cm^{-1} suggests that tiny ordered microdomains exist, which are out of the XRD detectable range, in the mechanically activated PMN–PMW compositions. Figure 6(b) shows the Raman spectra of a mechanically activated composition of 0.4PMN·0.6PMW when subjected to thermal annealing at increasing temperature, where the band intensity at around 384 cm^{-1} increases with increasing temperature. The split of the bands at 786 and 841 cm^{-1} becomes apparent when the annealing temperature is raised to 600°C.

To give a quantitative analysis of the relative intensity of order-sensitive bands, the bands enveloping at around 200–500 and 600–900 cm^{-1} in the Raman spectrum of 0.4PMN·0.6PMW can be fitted with a Gaussian function as shown in Fig. 7. The band envelopes can be deconvoluted into four bands centered at 278, 384, 786, and 841 cm^{-1}, and their corresponding relative intensities are expressed as I_{278}, I_{384}, I_{786}, and I_{841}, respectively. The relative intensity ratios of I_{384}/I_{278} and I_{841}/I_{786} for 0.4PMN·0.6PMW subjected to various hours of mechanical activation and thermal annealing at various temperatures are shown in Figs. 8(a,b). The I_{384}/I_{278} and I_{841}/I_{786} ratios decrease dramatically with increasing mechanical activation time from 1 to 5 h, due to the fall in degree of B-site ordering at the initial stage of mechanical activation. Further extension in mechanical activation time led to little change in the two ratios. On thermal annealing at increasing temperature as expected, I_{841}/I_{786} and I_{384}/I_{278} decrease sharply at temperatures around 600°C.

The order–disorder transition in PMN–PMW, as in many other ferroelectric compositions, is a rather complicated process and is affected by several structure and composition parameters. From the experimental results discussed above, it is apparent that the transition is composition dependent. Mechanical activation disorders the superlattice ordering in PMN–PMW, while subsequent thermal annealing can restore the ordering. Furthermore, the disordering triggered by mechanical activation takes place simultaneously with the refinement in crystallite size at the initial stage

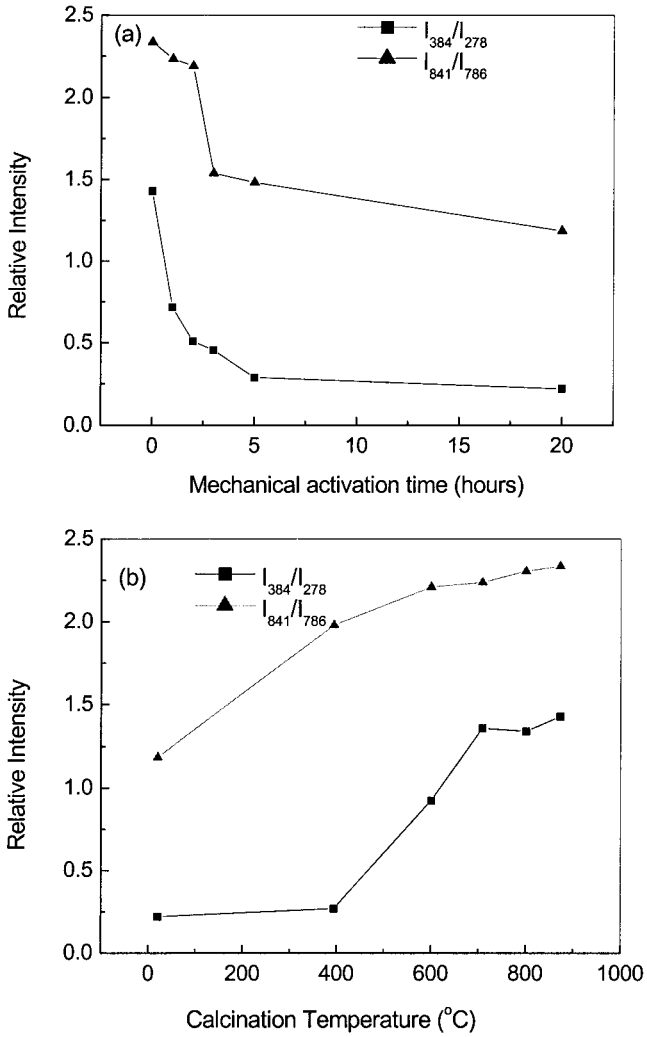

Fig. 8. Intensity ratios of I_{384}/I_{278}, I_{841}/I_{786} of 0.4PMN·0.6PMW, as a function of (a) activation time and (b) calcination temperature. I_{384}, I_{278}, I_{786}, and I_{841} represent the intensities of bands at 384, 278, 786, and 841 cm^{-1}, respectively.

of mechanical activation, apparently as a result of the fragmentation of crystallites. The process is thus similar to what has been observed for Fe–Al alloys,[21] where the shearing-induced glide causes the dwindling of ordered domains and thermal diffusion recovers the ordering. Although shear-induced glide may not occur in oxide-based ceramic materials at room temperature, it has been observed with a number of ceramic materials, including $BaTiO_3$ of perovskite structure and $La_{1-x}Sr_xMnO_3$, at elevated temperature.[30–32] This is especially so when the crystallite size is refined to nanometer scale, where the surface-related structure can dominate both the thermodynamic and kinetic processes. As has been clearly illustrated by the Raman spectra shown in Fig. 6, ordered microdomains existed in activated 0.4PMN·0.6PMW, which were not eliminated by up to 20 h of mechanical activation. The repeated mechanical impacting and shearing during mechanical activation fragmented the crystallites and ordered domains of PMN–PMW, which are shown by the broadening of principal peaks in both XRD and Raman spectra. On the other hand, the *in situ* temperature at the collision points, which is in the range of 400° to 500°C,[17,33–35] will contribute to the recovery of superlattice ordering. Therefore, the observed preservation of ordered microdomains in mechanically activated PMN–PMW compositions is a result of the equilibrium between the mechanical destruction of crystallites and domains and the recovering of ordering in association with the *in situ* temperature at collision points.

IV. Conclusions

Mechanical activation induces B-site disordering in PMN–PMW, where the refinements in ordered domain size and crystallite size occur simultaneously at the initial stage of mechanical activation. The order–disorder transition triggered by mechanical activation is composition dependent. B-site ordering of 0.4PMN·0.6PMW cannot be completely eliminated by mechanical activation, although XRD suggests otherwise. Tiny ordered microdomains existed in the composition subjected to 20 h of mechanical activation, as demonstrated by Raman spectroscopy. This was a result of the equilibrium between the mechanical destruction of ordered domains and crystallites and the recovery of ordering in association with in-site temperatures involved at the collision points during mechanical activation. The steady recovery of B-site ordering by thermal annealing occurred at around 600°C for PMN–PMW.

Acknowledgment

The authors thank Dr. C. B. Ponton of the School of Metallurgy and Materials, University of Birmingham, United Kingdom, for useful discussions and help with the TEM.

References

[1]N. Setter and L. E. Cross, "The Role of B Site Order in Diffuse Phase Transition Behavior of Perovskite Ferroelectrics," *J. Appl. Phys.*, **51** [8] 4356–60 (1980).
[2]N. Setter and L. E. Cross, "The Contribution of Structure Disorder to Diffuse Phase Transition in Ferroelectrics," *J. Mater. Sci.*, **15** [10] 2478–82 (1980).
[3]F. Chu and N. Setter, "The Spontaneous Relaxor–Ferroelectric Transition of $Pb(S_{0.5}Ta_{0.5})O_3$," *J. Appl. Phys.*, **74** [3] 5129–34 (1993).
[4]X. W. Zhang and Q. Wang, "Study of the Order–Disorder Transition in $A(B'B'')O_3$ Perovkite Type Ceramics," *J. Am. Ceram. Soc.*, **74** [11] 2846–50 (1991).
[5]H. M. Jang and S. C. Kim, "$Pb(B'_{1/2}B''_{1/2})O_3$-Type Perovskite: Part I, Pair-Correlation Theory of Order–Disorder Phase Transition," *J. Mater. Res*, **12** [8] 2117–26 (1997).
[6]P. K. Davies and M. A. Akbas, "Chemical Order in PMN-Related Relaxors: Structure, Stability, Modification, and Impact on Properties," *J. Phys. Chem. Solids*, **61** [2] 159–66 (2000).
[7]H. You and Q. M. Zhang, "Diffuse X-ray Scatterings Study of Lead Magnesium Niobate Single Crystals," *Phys. Rev. Lett.*, **79** [20] 3950–53 (1997).
[8]J. J. Fitzgerald, S. Prasad, J. Huang, and J. S. Shore, "Solid State ^{93}Nb NMR and ^{93}Nb Nutation Studies of Polycrystalline $Pb(Mg_{1/3}Nb_{2/3})O_3$ and $(1-x)Pb(Mg_{1/3}Nb_{2/3})O_3/xPbTiO_3$ Solid-Solution Relaxor Ferroelectrics," *J. Am. Chem. Soc.*, **122** [11] 2556–66 (2000).
[9]J. Huang, N. D. Chasteen, and J. J. Fitzgeral, "X-Band EPR Studies of Ferroelectric Lead Titanate (PT), Piezoeletric Lead Magnesium Niobate (PMN), and PMN/PT Powders at 10 K and 85 K," *Chem. Mater.*, **10** [12] 3848–55 (1998).
[10]I. G. Siny, S. G. Lushnikov and R. S. Katiyar, "Central Perak in Light Scattering from the Relxor Ferroelectric $Pb(Mg_{1/3}Nb_{2/3})O_3$," *Phys. Rev. B*, **56** [13] 7962–66 (1997).
[11]L. Bellaiche, J. Padilla, and D. Vanderbit, "Heterovalent and A-Atom Effects in $A(B'B'')O_3$ Perovskite Alloys," *Phys. Rev. B*, **59** [3] 1834–39 (1999).
[12]B. P. Burton and R. E. Cohen, "Nonempirical Calculation of $Pb(Sc_{0.5}Ta_{0.5})O_3$–$PbTiO_3$ Quasi-binary Phase Diagram," *Phys. Rev. B*, **52** [2] 792–97 (1995).
[13]A. D. Hilton and D. J. Barber, "On Short Range Ordering in the Perovskite Lead Magnesium Niobate," *J. Mater. Sci.*, **25** [8] 3461–66 (1990).
[14]H. C. Wang and W. A. Schuizer, "Order–Disorder Phenomenon in Lead Scandium Tantalate," *J. Am. Ceram. Soc.*, **73** [5] 1228–34 (1989).
[15]P. S. Gilman and J. S. Benjamin, "Mechanical Alloying," *Annu. Rev. Mater. Sci.*, **13**, 279–300 (1983).
[16]E. Gaffet, M. Addellaoui, and N. M. Gaffet, "Formation of Nanostruture Materials Induced by Mechanical Processings (Overview)," *Mater. Trans., Jpn. Inst. Met.*, **36** [2] 198–209 (1995).
[17]Wang, J. M. Xue, and D. M. Wang, "How Different Is Mechanical Activation from Thermal Activation? A Case Study with PZN and PZN-Based Relaxors," *Solid State Ionics*, **127**, 169–75 (2000).
[18]M. L. Trudeau and R. Schulz, "Structural Changes during High-Energy Ball Milling of Iron-Based Amorphous Alloys: Is High Energy Ball Milling Equivalent to a Thermal Process?," *Phys. Rev. Lett.*, **64** [1] 99–102 (1990).
[19]A. R. Yavari, P. J. Desre, and T. Benameur, "Mechanically Driven Alloying of Immiscible Elements," *Phys. Rev. Lett.*, **68** [14] 2235–38 (1992).
[20]Y. Chen, M. Bibole, R. Le Hazif, and G. Martin, "Ball-Milling-Induced Amorphization in Ni_xZr_y Compounds: A Parametric Study," *Phys. Rev. B*, **48** [1] 14–21 (1993).
[21]P. Pochet, E. Tominez, L. Chaffron, and G. Martin, "Order–Disorder Transformation in Fe–Al under Ball Milling," *Phys. Rev. B*, **52** [6] 4006–16 (1995).
[22]S. Nomura, S. L. Jang, L. E. Cross, and R. E. Newnham, "Structure and Dielectric Properties of Materials in the Solid Solution System $Pb(Mg_{1/3}Nb_{2/3})O_3$:$Pb(W_{1/2}Mg_{1/2})O_3$," *J. Am. Ceram. Soc.*, **62** [9–10] 485–88 (1979).

[23]H. P. Klug and L. E. Alexander, *X-ray Diffraction Procedures for Polycrystalline and Amorphous Materials*; pp. 491–538. Wiley, New York, 1954.

[24]N. Setter and L. Laulight, "The Observation of B-Site Ordering by Raman Scattering in $A(B'B'')O_3$ Perovskites," *Appl. Spectrosc.*, **41** [3] 526–28 (1987).

[25]U. Bismayer, V. Devarajan, and P. Groves, "Hard-Mode Raman Spectroscopy and Structural Phase Transition in the Relaxor Ferroelectric Lead Scandium Tantalite, $Pb(Sc_{0.5}Ta_{0.5})O_3$," *J. Phys. C*, **1**, 6977–86 (1989).

[26]G. A. Smolensky, I. G. Siny, R. V. Pisarev, and E. G. Kuzminov, "Raman Scattering in Ordered and Disordered Perovskite Type Crystals," *Ferroelectrics*, **12** [1–4] 135–36 (1976).

[27]I. G. Siny, R. S. Katiyar, and A. S. Bhalla, "Cation Arrengement in the Complex Perovskites and Vibrational Spectra," *J. Raman Spectrosc.*, **29**, 385–90 (1998).

[28]I. M. Reaney, J. Petzelt, V. V. Voitsekhovskii, F. Chu, and N. Setter, "B-Site Order and Infrared Reflectivity in $A(B'B'')O_3$ Complex Perovskite Ceramics," *J. Appl. Phys.*, **76** [4] 2086–92 (1994).

[29]C. A. Randall, D. J. Barber, R. W. Whatmore, and P. Groves, "A TEM Study of Ordering in Perovskite $Pb(Sc_{1/2}Ta_{1/2})O_3$," *J. Mater. Sci.*, **21** [12] 4456–62 (1986).

[30]C. Tromasy, J. C. Girard, and J. Wiorgard, "Study by Atomic Force Microscopy of Elementary Deformation Mechanisms Involved in Low Load Indentations in MgO Crystals," *Philos. Mag. A*, **80** [10] 2325–35 (2000).

[31]S. Maruyama, A. Gervais, and J. Philibert, "Transimission Electron Microscopy on Nickel Oxide Single Crystals Deformation on Room Temperature," *J. Mater. Sci.*, **17** [8] 2384–90 (1982).

[32]J. L. Routbort, K. C. Goretta, R. E. Cook, and J. Wolfenstine, "Deformation of Perovskite Electronic Ceramics—A Review," *Solid State Ionics*, **29** [1–4] 53–62 (2000).

[33]J. Wang, D. M. Wan, J. M. Xue, and W. B. Ng, Synthesizing $Pb(Zn_{1/3}Nb_{2/3})O_3$ Powders from Mixed Oxides," *J. Am. Ceram. Soc.*, **82**, 477–79 (1999).

[34]J. M. Xue, D. M. Wan, S. E. Lee, and J. Wang, Mechanochemical Synthesis of PZT from Mixed Oxides," *J. Am. Ceram. Soc.*, **82**, 1687–92 (1999).

[35]J. Wang, J. M. Xue, D. M. Wan, and B. K. Gan, "Mechanically Activating Nucleation and Growth of Complex Perovskites," *J. Solid State Chem.*, **154**, 321–28 (2000). □